Double vector quarkonia production in exclusive Higgs boson decays

V. Kartvelishvili,[1,*] A. V. Luchinsky,[2,†] and A. A. Novoselov[2,3]

[1]*Lancaster University, Lancaster, UK*
[2]*Institute for High Energy Physics, Protvino, Russia*
[3]*Moscow Institute of Physics and Technology, Dolgoprudny, Russia*

Partial decay widths and branching fractions are calculated for the exclusive decays of the standard model Higgs boson into a pair of vector quarkonium states, $H \to J/\psi J/\psi$, $H \to \Upsilon\Upsilon$, $H \to J/\psi \phi$, $H \to J/\psi \Upsilon$, with relativistic corrections due to quark motion in mesons taken into account.

I. INTRODUCTION

The necessary ingredient of the standard model (SM) is the Higgs boson—a scalar particle whose interactions are believed to generate masses of intermediate vector bosons and fundamental fermions. However, numerous attempts to discover this particle experimentally have so far only resulted in the limits on its possible mass M_H, 114.4 GeV $< M_H \lesssim 182$ GeV [1].

Decay modes that can be used to detect this particle depend on M_H. The coupling constant of the Higgs boson to another particle is known to be proportional to the mass of the latter, hence it is advantageous to search for Higgs boson decays into the heaviest of kinematically allowed particles. For instance, if M_H is above WW, ZZ production thresholds, $H \to WW$, ZZ decays (so-called "gold-plated" modes) can be used. Observation of such reactions is one of the main goals of the LHC physics program.

However, the possibility of $M_H < 2M_W$ cannot be excluded. In this case $b\bar{b}$ and $\tau^+\tau^-$ modes are dominant, but large backgrounds make these decays harder to observe. In search for an exclusive Higgs decay mode with a good signature, in [2–4] decays of the Higgs boson into a pair of heavy quarkonia ($H \to J/\psi J/\psi$, $\Upsilon\Upsilon$, $J/\psi\Upsilon$, etc.) were considered. The widths of such decays were found to be small, but their good signatures and high attainable mass resolutions could make these decays useful in certain circumstances.

The calculations in [2–4] were performed in the so-called δ approximation, i.e. they did not take into account relativistic corrections caused by the internal motion of quarks in the vector mesons. Since then, however, several theoretical and experimental studies of double charmonium production in exclusive processes have shown that the relativistic corrections can significantly alter the rates of these processes (see [5–9] for more details). In particular, the cross section of the reaction $e^+e^- \to J/\psi \eta_c$ is increased by about an order of magnitude [5–7]. Another

example is the decay $\chi_b \to J/\psi J/\psi$: in [7] it was shown that by taking the internal quark motion into account, the width of this decay increases by a factor of 3.

In this paper we study the influence of relativistic corrections on exclusive decays of the SM Higgs boson into a pair of vector quarkonia. The rest of the paper is organized as follows: in the next section we briefly describe the formalism used, and present the distribution amplitudes for various vector quarkonium states. In Sec. III analytical expressions are given for $H \to V_1 V_2$ decay amplitudes corresponding to leading contributing subprocesses. In Sec. IV we present numerical results for the Higgs decays into $V_1 V_2 = J/\psi J/\psi$, $\Upsilon(1S)\Upsilon(1S)$, $J/\psi \phi$, and $J/\psi \Upsilon(1S)$ final states, and compare them to the results obtained within the δ approximation. Our conclusions are given in the final section.

II. DISTRIBUTION AMPLITUDES

Consider double quarkonia production in exclusive Higgs boson decays

$$H \to V_1(p_1, \lambda_1) V_2(p_2, \lambda_2),$$

where $p_{1,2}$ and $\lambda_{1,2}$ are momenta and helicities of the two vector mesons, respectively. In what follows, we restrict ourselves to leading twist approximation. It can be shown (see, for example, [10–14] for details) that in this approximation final state mesons should be longitudinally polarized, i.e $\lambda_{1,2} = 0$, as transversely polarized components are suppressed by a small factor $\sim \mathcal{O}(M_V/M_H)$.

The transition of a quark-antiquark pair into a longitudinally polarized vector meson is described by the expression

$$\langle V(p, \lambda = 0)|\bar{q}^i_\alpha(z) q^j_\beta(-z)|0\rangle$$
$$= \frac{f}{4}\frac{\delta^{ij}}{3}(\not{p})_{\alpha\beta}\int_0^1 dx \varphi(x) e^{i(2x-1)pz}, \quad (1)$$

where α (β) and i (j) are spinor and color indices of the antiquark (quark), respectively, while x is the quark momentum fraction with respect to the meson momentum. The constant f can be determined from the leptonic width of the vector meson

*V.Kartvelishvili@lancaster.ac.uk
†Alexey.Luchinsky@ihep.ru
‡Alexey.Novoselov@cern.ch

$$\Gamma(V \to e^+ e^-) = \frac{4\pi\alpha^2}{3} e_q^2 \frac{f^2}{M}, \quad (2)$$

where α is the fine structure constant, e_q is the quark charge (2/3 for J/ψ, $-1/3$ for ϕ and Υ), and M is the mass of quarkonium.

A distribution amplitude $\varphi(x)$, describing the internal motion of the heavy quark-antiquark pair inside their bound state, can generally be written as a series of Gegenbauer polynomials $C_n^{3/2}$ [10]

$$\varphi(x, \mu) = 6x\bar{x}\left[1 + \sum_{n=2,4,\ldots} a_n(\mu)C_n^{3/2}(x - \bar{x})\right], \quad (3)$$

where we have introduced a simplifying notation $\bar{x} = 1 - x$. The dependence of this distribution on energy scale μ is described by the QCD evolution of the moments $a_n(\mu)$

$$a_n(\mu) = \left(\frac{\alpha_s(\mu)}{\alpha_s(\mu_0)}\right)^{\gamma_n} a_n(\mu_0), \quad (4)$$

with the anomalous dimensions γ_n defined by

$$\gamma_n = \frac{4}{3b_0}\left(1 - \frac{2}{(n+1)(n+2)} + 4\sum_{j=2}^{n+1}\frac{1}{j}\right), \quad (5)$$

$$b_0 = 11 - \frac{2}{3}n_f, \quad (6)$$

where n_f is the number of active quark flavors. These anomalous dimensions are positive, so in the limit $\mu \to \infty$ (or, equivalently, for light mesons) moments (4) tend to zero. As a result, in this limit distribution amplitude (3) tends to its asymptotic form $\varphi_a(x) = 6x\bar{x}$. We use this form of the distribution amplitude for the ϕ meson.

However, for heavier quarkonia J/ψ and Υ and for the scales $\mu = M_H \sim 100$–250 GeV, the asymptotic limit is not reached yet. Following [15], for J/ψ we use the distribution amplitude

$$\varphi_{J/\psi}(x, m_c) = c(\beta)(1 - (x - \bar{x})^2)\exp\left\{-\frac{\beta}{1 - (x - \bar{x})^2}\right\}, \quad (7)$$

with $\beta \approx 3.8$ and the factor $c(\beta)$ fixed from the normalization condition

$$\int_0^1 \varphi(x)dx = 1.$$

Note that this function is fairly close to a simpler expression [16,17]

$$\varphi_{J/\psi}(x) \sim x^{-\alpha_\psi}\bar{x}^{-\alpha_\psi}, \quad (8)$$

where $\alpha_\psi \simeq -3$ is the intercept of the Regge trajectory corresponding to charmonium. For the wave function of Υ we use a parametrization similar to (8) with the intercept $\alpha_\Upsilon = -9$ [17]. The typical scale μ for these distribution amplitudes is the corresponding quark mass. Using formu-

lae (3)–(5), their evolution to $\mu = M_H$ can be easily calculated.

III. $H \to V_1 V_2$

Typical diagrams that give leading contributions to $H \to V_1 V_2$ decays are shown in Fig. 1.

For the diagram shown in Fig. 1(a), only Z will contribute as the intermediate virtual bosons, as the final mesons should be neutral and colorless. On the other hand, in this subprocess the two final mesons can be composed from different types of quarks. The corresponding amplitude is

$$\mathcal{M}^{(ZZr)} = -\left[\frac{e}{\sin 2\vartheta_W}\right]^3 \frac{a_1 f_1}{D_Z(M_1^2)} \frac{a_2 f_2}{D_Z(M_2^2)} M_H^2 M_Z. \quad (9)$$

Here ϑ_W is the Weinberg angle, $D_Z(M) = M^2 - M_Z^2 + iM\Gamma_Z$ is the inverse propagator of the virtual Z boson,
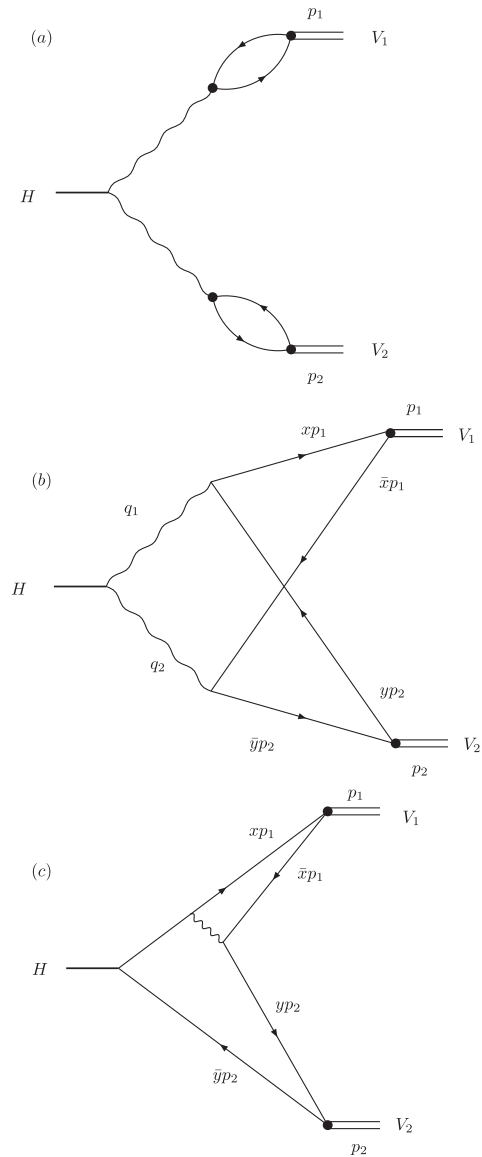

FIG. 1. Typical diagrams describing $H \to V_1 V_2$ decays.

and constants $a_{1,2}$ are defined as

$$a_i = \pm\frac{1}{2} - 2e_q\sin^2\vartheta_W,$$

with the $+$ $(-)$ sign used for c (s, b) quarks. One can see that this amplitude is expressed through experimentally observable quantities only, and hence does not depend on distribution functions $\varphi(x)$. Note also that this amplitude increases with increasing Higgs boson mass.

The situation is rather different for the subprocess described by the diagram in Fig. 1(b). In this case, either Z, W, or gluons can be used as virtual particles. Their momenta can be calculated as

$$q_1 = xp_1 + yp_2, \qquad q_2 = \bar{x}p_1 + \bar{y}p_2,$$

where $p_{1,2}$ are the momenta of final vector mesons, x and y are momentum fractions of quarks inside V_1 and V_2, respectively, while $\bar{x} \equiv 1 - x$, and $\bar{y} \equiv 1 - y$. So, neglecting the masses of the quarkonia compared to $M_{W,Z}$ and M_H, the virtualities of the intermediate bosons are

$$q_1^2 = 2xy(p_1p_2) = xyM_H^2, \qquad q_2^2 = \bar{x}\,\bar{y}\,M_H^2.$$

Clearly, in contrast with the previous diagram, these amplitudes depend on the distribution functions $\varphi_{1,2}(x)$. In addition, they do not increase with the increasing Higgs boson mass.

In the case of ZZ decay, the quarks in mesons should be the same. The amplitude is equal to

$$\mathcal{M}^{(ZZ)} = -\frac{1}{3}\left[\frac{e}{\sin2\vartheta_W}\right]^3 b_q M_H^2 f_1 f_2 M_Z$$
$$\times \int_0^1 dxdy \frac{\varphi_1(x)}{D_Z(xyM_H^2)}\frac{\varphi_2(y)}{D_Z(\bar{x}\,\bar{y}\,M_H^2)}, \quad (10)$$

where

$$b_q = \frac{1}{2} \mp 2e_q\sin^2\vartheta_W + 4e_q^2\sin^4\vartheta_W$$

and the upper (lower) sign corresponds to mesons built from up- (down-) type quarks. In the limit of large M_H this amplitude remains constant. In the region $M_H \approx 2M_Z$, however, there is a noticeable peak, because in this case, due to the specific kinematics of the quarkonium formation, both intermediate Z bosons are bound to be close to their mass shell.

If the decay in Fig. 1(b) is mediated by a pair of W bosons, quarks in different mesons should be different, with one of the mesons built from up-type quarks, while the other from down-type quarks. Here we consider $J/\psi\phi$ and $\Upsilon J/\psi$ final states. The amplitude of such a decay is equal to

$$\mathcal{M}^{(WW)} = -\frac{1}{24}\frac{e^3\cot\vartheta_W}{\sin^2\vartheta_W}|V_{12}|^2 M_H^2 f_1 f_2 M_Z$$
$$\times \int_0^1 dxdy \frac{\varphi_1(x)}{D_W(xyM_H^2)}\frac{\varphi_2(y)}{D_W(\bar{x}\,\bar{y}\,M_H^2)}, \quad (11)$$

where V_{12} is the respective Cabibbo-Kobayashi-Maskawa matrix element, while $D_W(M) = M^2 - M_W^2 + iM\Gamma_W$ is the inverse propagator of a virtual W boson. This amplitude also has a peak, this time at $M_H \approx 2M_W$.

In the case of gg intermediate state, quark content of the vector mesons should again be the same. In the standard model there is no $H \to gg$ coupling at tree level, but it appears at higher orders when loop diagrams are taken into account. The main contribution to this effective vertex comes from the top quark loop, for which we use the expression (see, e.g., [18])

$$\mathcal{M}(H \to gg) = \frac{\alpha_s(M_H)}{6\pi}\frac{e}{\sin2\theta_W M_Z}G_{\mu\nu}^{1a}G_{\mu\nu}^{2a},$$

where the tensor $G_{\mu\nu}$ is defined according to

$$G_{\mu\nu}^{ia} = q_{i\mu}\epsilon_{i\nu} - q_{i\nu}\epsilon_{i\mu}.$$

Strictly speaking, the value of the strong coupling constant in this vertex depends on gluon virtualities, but this dependence is only logarithmic and we do not take it into account. Using this effective vertex, we obtain the following expression for $H \to gg \to V_1V_2$ decay amplitude:

$$\mathcal{M}^{(gg)} = -\frac{\sqrt{2}}{27}\frac{e\tan\vartheta_W\alpha_s(M_H)}{M_Z}f_1 f_2$$
$$\times \int_0^1 dxdy\varphi_1(x)\varphi_2(y)\left[\frac{1}{x\bar{y}} + \frac{1}{y\bar{x}}\right]. \quad (12)$$

Clearly, this amplitude only depends on the Higgs boson mass through α_s.

There are other subprocesses contributing to the same double quarkonium final states, notably those containing the tree-level vertex $H \to \bar{q}q$ shown in Fig. 1(c), first calculated in [2]. In such subprocesses, the two quarkonia must again be the same, and the amplitude can be written as

$$\mathcal{M}^{(qq)} = \frac{\pi\alpha_s}{9}\frac{M_V^2}{M_Z}\frac{f_1 f_2}{M_H^2}\int_0^1 dxdy\frac{\varphi_1(x)\varphi_2(y)}{\bar{x}y}\left[\frac{1}{\bar{x}} + \frac{1}{y}\right].$$

Compared to other amplitudes considered above, in the Higgs mass range of interest this amplitude is suppressed by a small factor $(M_V/M_H)^2$, so we will neglect it in the following.

IV. NUMERICAL RESULTS

In order to obtain numerical results from Eqs. (9)–(12), one needs the values for constants f and the distribution amplitudes $\varphi(x)$. The constants f, as determined from the

leptonic decay widths $V \to e^+e^-$ using Eq. (2), yield $f = 200$ MeV, 400 MeV, and 700 MeV for ϕ, J/ψ, and $\Upsilon(1S)$ mesons, respectively. Our choices for the distribution amplitudes of these three vector mesons were given by Eqs. (3), (7), and (8), respectively. After fixing these, calculations of partial decay widths for the decays $H \to V_1 V_2$ are fairly straightforward.

As an example, in Fig. 2 we show M_H dependence of various amplitudes contributing to the decay $H \to J/\psi J/\psi$. The amplitudes calculated with internal quark motion taken into account are shown with solid lines, while for dashed lines this motion is neglected. In δ approximation, the amplitude of the subprocess $H \to ZZ \to J/\psi J/\psi$ has a prominent peak at $M_H = 2M_Z$ (dashed line labeled ZZ). The reason for this peak, as explained above, is that at this value of the Higgs mass both virtual Z bosons in Fig. 1 (b) are on mass shell. When the internal quark motion is taken into account, the quark momentum fractions x, y are allowed to deviate from $1/2$, and the Z bosons are off mass shell. As a result, the peak is washed out, while away from the peak the amplitude becomes somewhat larger (solid line). The amplitude of the subprocess shown in Fig. 1(a) (solid line labeled ZZr) remains unchanged when the internal quark motion is taken into account. As for the gluon-gluon subprocess (solid and dashed lines labeled gg), internal quark motion increases the corresponding amplitude roughly by a factor of 2.

The main features of the above analysis hold also for other decays considered here. Using the total width of the Higgs boson, calculated following [19], one obtains the branching fractions of these decays. Their dependence on the Higgs boson mass is shown in Fig. 3. Solid (dashed) lines in this figure correspond to internal quark motion taken into account (neglected). One can see that the resonant peaks at $M_H = 2M_{Z,W}$, prominent in the δ approximation, are significantly smeared out once internal quark motion is accounted for. For Higgs boson masses away from these peaks, relativistic corrections increase the widths of the decays.
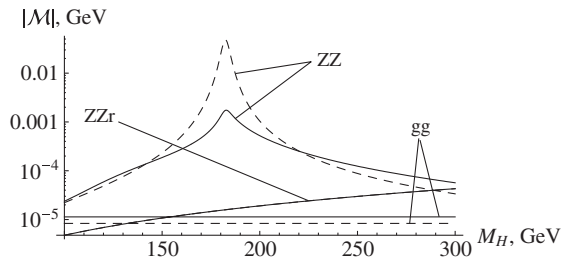
FIG. 3. Branching fractions (Br) of the exclusive decays $H \to V_1 V_2$ versus the Higgs boson mass, with internal quark motion taken into account (solid lines) and neglected (dashed lines): from top to bottom, the final states are $J/\psi J/\psi$, $\Upsilon\Upsilon$, $J/\psi\phi$ and $J/\psi\Upsilon$.

V. CONCLUSION

We have calculated the partial decay widths and branching fractions for the exclusive decays of the standard model Higgs boson into a pair of vector quarkonium states, $H \to J/\psi\phi$, $H \to J/\psi J/\psi$, $H \to J/\psi\Upsilon$, $H \to \Upsilon\Upsilon$, with relativistic corrections due to quark motion in mesons taken into account, and compared our results with previous calculations performed in δ approximation. We have found that the characteristic increases of the respective decay probabilities at $M_H = 2M_{Z,W}$ are still noticeable, but the relativistic corrections make them far less pronounced. For M_H away from that resonant area, relativistic corrections result in an increase of the branching fractions by factors ranging from about 2 to 10 and above, depending on the specific decay mode and the value of the Higgs mass.

FIG. 2. Amplitudes of different subprocesses contributing to the decay $H \to J/\psi J/\psi$ versus the Higgs boson mass. Solid (dashed) lines stand for internal quark motion taken into account (neglected). See text for further explanation.
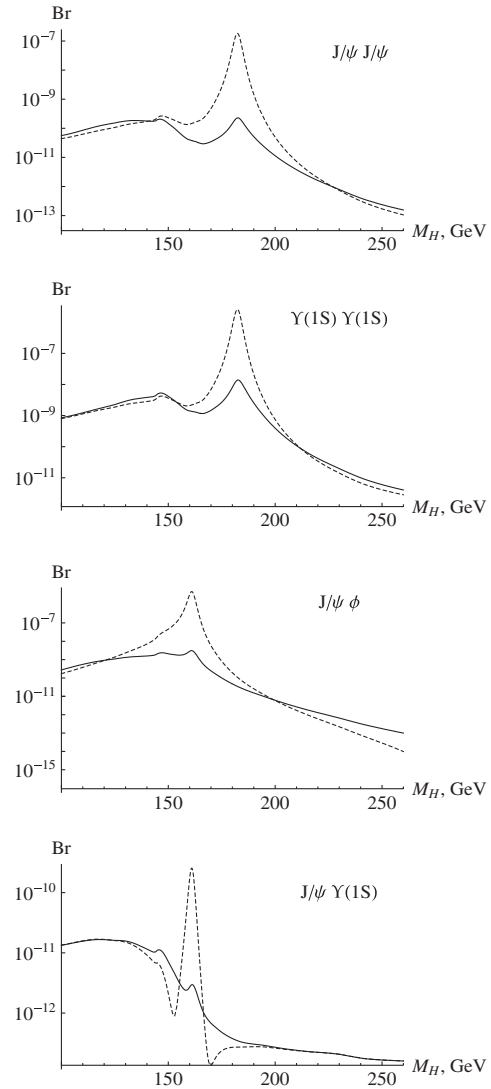
However, the decay probabilities remain fairly small, and further studies are needed to identify possible areas where these decays may be useful experimentally.

ACKNOWLEDGMENTS

[1] C. Amsler *et al.* (Particle Data Group), Phys. Lett. B **667**, 1 (2008).

[2] W. Y. Keung, Phys. Rev. D **27**, 2762 (1983).

[3] M. N. Doroshenko, V. G. Kartvelishvili, E. G. Chikovani, and S. M. Esakiya, Yad. Fiz. **46**, 864 (1987).

[4] V. G. Kartvelishvili, E. G. Chikovani, and S. M. Esakiya, Fiz. Elem. Chastits At. Yadra **19**, 139 (1988).

[5] K. Abe *et al.* (Belle Collaboration), Phys. Rev. Lett. **89**, 142001 (2002).

[6] A. E. Bondar and V. L. Chernyak, Phys. Lett. B **612**, 215 (2005).

[7] V. V. Braguta, A. K. Likhoded, and A. V. Luchinsky, Phys. Rev. D **72**, 094018 (2005).

[8] V. V. Braguta, A. K. Likhoded, and A. V. Luchinsky, Phys. Rev. D **72**, 074019 (2005).

[9] V. V. Braguta, A. K. Likhoded, and A. V. Luchinsky, Phys. Lett. B **635**, 299 (2006).

[10] V. L. Chernyak and A. R. Zhitnitsky, Phys. Rep. **112**, 173 (1984).

[11] S. J. Brodsky and G. P. Lepage, Phys. Rev. D **24**, 2848 (1981).

[12] V. L. Chernyak, A. R. Zhitnitsky, and V. G. Serbo, Pis'ma Zh. Eksp. Teor. Fiz. **26**, 760 (1977) [JETP Lett. **26**, 594 (1977)].

[13] V. L. Chernyak and A. R. Zhitnitsky, Yad. Fiz. **31**, 1053 (1980) [Sov. J. Nucl. Phys. **31**, 544 (1980)].

[14] V. L. Chernyak and A. R. Zhitnitsky, Pis'ma Zh. Eksp. Teor. Fiz. **25**, 544 (1977) [JETP Lett. **25**, 510 (1977)].

[15] V. V. Braguta, Phys. Rev. D **75**, 094016 (2007).

[16] V. G. Kartvelishvili and A. K. Likhoded, Yad. Fiz. **42**, 1306 (1985) [Sov. J. Nucl. Phys. **42**, 823 (1985)].

[17] S. S. Gershtein, A. K. Likhoded, and A. V. Luchinsky, Phys. Rev. D **74**, 016002 (2006).

[18] L. B. Okun, *Leptons and Quarks* (North-Holland, Amsterdam, 1982).

[19] A. Djouadi, J. Kalinowski, and M. Spira, Comput. Phys. Commun. **108**, 56 (1998).